

This is the peer reviewed version of the following article: Torabi M, Rosychuk RJ (2012). Hierarchical Bayesian Spatio-temporal Analysis of Childhood Cancer Trends. *Geographical Analysis*, 44, 109-120., which has been published in final form at <http://onlinelibrary.wiley.com/doi/10.1111/j.1538-4632.2012.00839.x/abstract>. This article may be used for non-commercial purposes in accordance with Wiley Terms and Conditions for Self-Archiving.

Hierarchical Bayesian Spatio-Temporal Analysis of Childhood Cancer Trends

Mahmoud Torabi,¹ Rhonda J. Rosychuk²

¹ Department of Community Health Sciences, University of Manitoba, Winnipeg, Canada, ² Department of Pediatrics, University of Alberta, Edmonton, Canada

In this paper, generalized additive mixed models are constructed for the analysis of geographical and temporal variability of cancer ratios. In this class of models, spatially correlated random effects and temporal components are adopted. Spatio-temporal models that use intrinsic conditionally autoregressive smoothing across the spatial dimension and B-spline smoothing over the temporal dimension are considered. We study the patterns of incidence ratios over time and identify areas with consistently high ratio estimates as areas for further investigation. A hierarchical Bayesian approach using Markov chain Monte Carlo techniques is employed for the analysis of the childhood cancer diagnoses in the province

of Alberta, Canada during 1995-2004. We also evaluate the sensitivity of such analyses to prior assumptions in the Poisson context.

Introduction

For children aged one year to adolescence in Canada, childhood cancer leading to death outnumbers any other disease-specific deaths; it causes more deaths than asthma, diabetes, cystic fibrosis and AIDS combined (Borugian et al. 2005). Given this outcome, analyzing the ratio of childhood cancer diagnoses based on geographical and temporal variations is worthwhile. We consider spatial and temporal trends in the annual number of childhood cancer diagnoses between 1995 and 2004 in the province of Alberta, Canada.

The analysis of disease ratios over region and time has received considerable attention because of the desire to provide reliable maps of disease ratios. Maps of regional incidence ratios over time are useful tools in determining spatial and temporal patterns of disease. Disease incidence ratios may differ substantially across geographical regions. Evaluating such spatial variation in a disease by regional characteristics may provide important information to determine the risks and causes of the disease.

The analysis of disease cases over space uses Poisson regression, which

implicitly assumes that the cases in nearby regions are independent and the variance of cases is equal to the mean. However, these may not be reasonable assumptions because unmeasured casual factors of a disease that are omitted from a regression model can lead to extra-Poisson variation. In addition, a certain degree of spatial correlation may be present in a response, depending on how smoothly the omitted factors vary across regions. The use of mixed models for geographical data to account for extra-Poisson variability through the introduction of random effects was first used by Clayton and Kaldor (1987); often the random effects are spatially correlated in a disease mapping context. For inference based on mixed models, one may use empirical Bayes or Markov chain Monte Carlo (MCMC) methods such as the Gibbs sampler (Besag, York, and Mollié 1991; Bernardinelli and Montomoli 1992; Clayton and Bernadinelli 1992; Cressie 1992; Waller et al. 1997; Knorr-Held 2000; Lu and Carlin 2005). Breslow and Clayton (1993) propose the use of the penalized quasi-likelihood (PQL) method for inference in generalized linear mixed models (GLMMs), and also provide an example in the context of disease mapping. The PQL method has been used extensively in the literature (Breslow and Lin 1995; Lin and Breslow 1996; MacNab and Dean 2000, 2001; Dean, Ugarte, and Militino 2004). The generalized estimating equation (GEE) approach, introduced by Liang and Zeger (1986) and Prentice and Zhao (1991), also may be used for inference in GLMMs.

The temporal random smoothing of ratios also has been studied in the literature. Zeger (1988) uses an autoregressive (AR) model to describe temporal count data. Waller et al. (1997) extend the existing hierarchical Bayesian spatial models to account for temporal random effects and spatio-temporal interactions. Knorr-Held (2000) proposes a unified approach for a Bayesian analysis of incidence or mortality data in space and time. MacNab and Dean (2001) and Silva et al. (2008) propose spatio-temporal models that use AR local smoothing across the spatial effects, and B-spline smoothing over the temporal effects. Martinez-Beneito, López-Quilez, and Botella-Rocamora (2008) suggest an autoregressive spatio-temporal model based on time series and Bayesian spatial modeling to link information in time and space.

To fit an appropriate model for our dataset of childhood cancer incidence, we study a comprehensive model that is based on a generalized additive mixed model (GAMM) to account for the spatio-temporal analysis of risks. This model accommodates spatially correlated random effects and temporal effects. The well-known intrinsic conditionally autoregressive (ICAR) approach (Besag, York, and Mollié 1991) is used for the spatial random effects, and linear trend and B-spline approaches are used for the temporal effects. The model specification also accommodates the interaction between space and time.

Methodology

Let y_{it} be the number of disease cases for the i -th geographic area at year t , and let e_{it} be the corresponding expected number of disease cases for $i = 1, \dots, I; t = 1, \dots, T$. Define μ_{it}^c as the conditional expectation of the y_{it} given the random effects. A generalized Poisson mixed model for μ_{it}^c is given by

$$\mu_{it}^c = \exp[\log(e_{it}) + m + S(t) + \eta_i + \phi_i + \theta_{it}], \quad (1)$$

where m is a fixed effect representing the overall mean ratio over time and region, η_i and ϕ_i represent specified and unspecified features of the spatial structure of area i , respectively, and θ_{it} is the interaction between the spatial and temporal effects. To account for the fixed temporal effects, $S(t)$ represents a cubic B-spline with three inner knots (Eilers and Marx 1996), a specification found useful in our exploration of the data. Note that the knots are located in the first and third quartiles as well as the median of time t ($= 1, \dots, T$). For example, if $T = 10$, the knots would be located at $t = 3.25, 5.50$, and 7.75 . One may simply consider a linear trend (βt) instead of $S(t)$, depending on the nature of a dataset. With the overall mean of ratio m in our model, the B-spline is provided without an intercept. In this case, $S(t)$ is given by

$$S(t) = \beta_1 B_1(t) + \beta_2 B_2(t) + \beta_3 B_3(t) + \beta_4 B_4(t),$$

where (β_l, B_l) are the coefficients and basis functions of the B-spline, respectively ($l = 1, \dots, 4$), with $B_l(t)$ being a cubic function of t (De Boor 1978; Eilers and Marx 1996).

To capture the random effects η_i , the usual ICAR model is used. One may define a variety of ICAR models by taking a collection of mutually compatible conditional distributions $p(\eta_i|\eta_{-i})$, $i = 1, \dots, I$, where $\eta_{-i} = \{\eta_j; j \neq i, j \in \partial_i\}$ and ∂_i denotes a set of neighbours for the i -th area (Besag, York, and Mollié 1991). In particular, we define the following model for the spatial effects η_i :

$$\eta = (\eta_1, \dots, \eta_I)' \sim N(0, \Sigma_\eta),$$

$$\Sigma_\eta = \sigma_\eta^2 \mathbf{D}^{-1},$$

where σ_η^2 is the spatial dispersion parameter. The neighbourhood matrix \mathbf{D} is defined such that its i -th diagonal element is the number of neighbours of the corresponding area (∂_i), and the off-diagonal elements in each row are -1 if the corresponding areas are neighbours and zero otherwise (Leroux, Lei, and Breslow 1999; MacNab and Dean 2000, 2001). Because \mathbf{D} is a singular matrix, one may use the Moore-Penroze generalized inverse \mathbf{D}^{-1} (Harville 1997). One can define the neighbours matrix \mathbf{D} in various ways (Earnest et al. 2007), depending on the context of an analysis, but one popular definition is simply the set of areas that have common borders, and

we use this definition. We have $\eta_i|\eta_{-i} \sim N(\bar{\eta}, \sigma_\eta^2/\partial_i)$ by noting that $\bar{\eta}$ is the mean of the random effects in the neighbourhood of the i -th area.

The unstructured heterogeneity $\phi = (\phi_1, \dots, \phi_I)'$ is assumed to have a Gaussian distribution with mean 0 and covariance matrix $\sigma_\phi^2 I_I$, where I_I is an identity matrix with dimension I .

One may define the interaction effect of space and time, θ_{it} , as $\delta_i t$ or $S_i(t)$ depending on the nature of a dataset (Bernardinelli et al. 1995; MacNab and Dean 2001; Silva et al. 2008), where δ_i is the coefficient of the linear temporal effect related to the i -th area, and $S_i(t)$ is a cubic B-spline for specific area i .

Bayesian inference and model comparison

With advances in computational power, much progress in empirical Bayes and Bayesian hierarchical modeling has been made that enables stable estimators for mortality rates in small areas by using information from all areas to derive estimates for individual areas. A comprehensive account of hierarchical Bayesian (HB) models for spatial and spatio-temporal data is given by Banerjee, Carlin, and Gelfand (2004).

We employ the Bayesian approach using MCMC to estimate the model parameters (say ω). In the HB approach, we estimate ω by its posterior mean.

The uncertainty in the HB estimate is measured by the posterior standard deviation of ω . We use the Gibbs sampler (e.g., Gelfand and Smith 1990; Gelman and Rubin 1992) to obtain the posterior mean and posterior variance of ω . The Gibbs sampler is a Monte Carlo Markovian updating scheme that gives the marginal, conditional, and joint distribution of the random variables v_1, \dots, v_s (say), where s is the length of ω . The joint density of v_1, \dots, v_s is assumed to be equally determined by the collection of conditional densities of v_r given $v_{-r} = (v_1, \dots, v_{r-1}, v_{r+1}, \dots, v_s)'$, and $f(v_r|v_{-r}), r = 1, \dots, s$. The Gibbs sampler requires generation of samples from the conditional densities $f(v_r|v_{-r})$ for $r = 1, \dots, s$. Starting with an initial set of values $v_1^{(0)}, \dots, v_s^{(0)}$, a random number, $v_1^{(1)}$, is first generated from $f(v_1|v_{-1}^{(0)})$. In a similar way, we generate $v_2^{(1)}, \dots, v_s^{(1)}$ successively from $f(v_2|v_1^{(1)}, v_3^{(0)}, \dots, v_s^{(0)}), \dots, f(v_s|v_{-s}^{(1)})$. Hence, the first replicate $v_1^{(1)}, \dots, v_s^{(1)}$ is obtained. We continue replicating, say R times, where $(v_1^{(R)}, \dots, v_s^{(R)})$ converges to (v_1, \dots, v_s) in distribution under some regularity conditions.

To generate samples from the posterior distribution using the MCMC method via the Gibbs sampler, we need to sample from the full conditional distributions. In our application, all of these full conditional distributions are standard distributions that can be easily sampled. To implement our application in the HB setup, we use the WinBUGS software (Lunn et al.

2000). We use the ICAR for spatial random effects as previously defined. The hyperparameters σ_η^2 and σ_ϕ^2 , which determine the variation of the spatial model, have to be estimated from the data. We assign the proper gamma distributed priors to the precision of spatial effects, $(\sigma_\eta^{-2}, \sigma_\phi^{-2})$, where the proper gamma is given by $\sigma^{-2} \sim G(a, b)$ (say), with mean a/b and variance a/b^2 , to avoid problems with improper hyperpriors. Gamma distributed priors are computationally convenient as the full conditional of σ^{-2} again is gamma distributed. Moreover, if a linear trend $\theta_{it} = \delta_i t$ is postulated, one may assume that $\delta_i \sim N(0, \sigma_\delta^2), i = 1, \dots, I$, independently, and independent of spatial random effects η_i and ϕ_i , where σ_δ^{-2} is assigned a proper gamma distributed prior. When considering a linear trend (βt) as the overall temporal trend, β would be assigned an independent normal distribution with zero mean and a large variance. When considering a cubic B-spline for $S(t)$ and θ_{it} , the corresponding B-spline basis functions β_l and β_{li} are assigned independent normal distributions with zero means and variances σ_l^2 and $\sigma_l^{2*}(i = 1, \dots, I; l = 1, \dots, 4)$, where proper gamma distributed priors are designated for σ_l^{-2} and σ_l^{-2*} . The gamma distributed priors as well as the normal distributed priors are usually assigned highly dispersed, but proper, priors.

In terms of prior assumptions, we assign a flat prior for the whole real line

for m and highly dispersed priors for all other model parameters, where flat prior means that each point in real line has an equal chance to be chosen. In particular, we assign $N(0, 10^6)$ for β , $N(0, \sigma_\delta^2)$ for δ_i , $N(0, \sigma_l^2)$ and $N(0, \sigma_l^{2*})$ for the coefficients of the B-spline β_l and β_{li} parameters, and $G(0.5, 0.0005)$ for the spatial hyperparameters σ_η^{-2} , σ_ϕ^{-2} , and σ_δ^{-2} , σ_l^{-2} , σ_l^{-2*} ($l = 1, \dots, 4$).

In order to ensure that the ICAR model is identifiable, Besag and Kooperberg (1995) suggest constraining the random effects to sum to zero, and using a flat prior for the entire real line for the intercept, m . For more details about the choice of hyperparameters in disease mapping, see Bernardinelli, Clayton, and Montomoli (1995) and the discussion in Best et al. (1999).

For each model considered in the subsequent Application section, we independently simulate $l = 5$ parallel runs, each of length $D = 2d$, with $d = 5,000$. To reduce the effects of the starting values on the final results, the first 5,000 iterations of each run are deleted (a burn-in sequence). We take every 5th iteration of the remaining 5,000 iterations to reduce the autocorrelation in the run (i.e., thinning or weeding), leading to 1,000 iterations for each run for analysis purposes. Hence, we have $l = 5$ runs with sample size $n = 1,000$ for each run. To monitor the convergence of the model parameters, we use several diagnostic methods implemented in the Bayesian output analysis (BOA) program (Smith 2007), a freely available package created for R. In particular,

we evaluate descriptive diagnostic tests, such as the autocorrelation of generated samples of model parameters from the posterior distribution, and convergence diagnostic tests, such as the Brooks, Gelman, and Rubin test (Gelman and Rubin 1992; Brooks and Gelman 1998) and the Heidelberger and Welch (1983) test. None of these tests indicated non-convergence of the model parameters.

An important aspect of our analysis is the choice of the best model among postulated sub-models of model (1). Unfortunately, some criteria are not applicable (e.g., Bayes factor) to the model in the presence of flat or ICAR priors. Some measures of model comparison may be calculated easily with MCMC methods. In the context of a Poisson likelihood function, we have three criteria that we compare in our application. The first criterion is the *saturated deviance* (McCullagh and Nelder 1989), defined as

$$SD = \sum_{i=1}^I \sum_{t=1}^T d_{it},$$

where

$$d_{it} = 2\{y_{it} \log(\frac{y_{it}}{\hat{\mu}_{it}^c}) - y_{it} + \hat{\mu}_{it}^c\}.$$

The second measure is the *Pearson function* (McCullagh and Nelder 1989), defined as

$$P = \sum_{i=1}^I \sum_{t=1}^T (y_{it} - \hat{\mu}_{it}^c)^2 / \hat{\mu}_{it}^c.$$

The last measure is the *deviance information criterion* (DIC), which is a standard measure in the Bayesian setup (Spiegelhalter et al. 2002). This measure is a generalization of the Akaike information criterion, which handles hierarchical Bayesian models of any degree of complexity. It is given by

$$DIC = 2\overline{SD(\omega)} - SD(\bar{\omega}),$$

where $\overline{SD(\omega)}$ is the posterior mean of the saturated deviance, and $\bar{\omega}$ is the posterior mean of the model parameter vector ω . Although we mainly rely on this measure for assessing models in our application, the other measures also are computed for comparison purposes. Smaller values of the above criteria indicate a better model in terms of fit and complexity.

The DIC can be partitioned into the local DIC, leverage, and deviance residuals to assess the local model fit and influence by visualization for groups of observations (Wheeler, Hickson, and Waller 2010). However, in this paper we focus on the DIC proposed by Spiegelhalter et al. (2002).

An application

A dataset of all cancer diagnoses in children (age ≤ 19) in the western Canadian province of Alberta during 10 fiscal years is considered in this cohort, which corresponds to $T = 10$ in our notation. The cohort includes

all children and youth residing in Alberta with any type of cancer diagnosis during April 1, 1994, to March 31, 2004.

The Alberta Cancer Registry is a population-based registry certified by the North American Association of Central Cancer Registries (NAACCR). Generally, the certification is at the “Gold” level, which means that certain standards have been achieved, such as at least 95% completion of case ascertainment, fewer than 0.1% duplicate cases, and variables to provide incidence statistics are 100% error free. Full details about the certification are available at www.naacrr.org/Certification/CertificationLevels.aspx.

Data extracted from the Registry included sex (female, male, other), age year at diagnosis (0-19 years), calendar year and fiscal year of diagnosis, morphology and topography codes, and behaviour code (benign, undetermined, in situ, malignant). During the study period, the population of Alberta increased from 2.7 million in 1995 to 3.2 million in 2004, and the average annual population of children numbered approximately 800,000. During the last study year, the province consisted of nine Regional Health Authorities that were responsible for the delivery of health care services. These regions are further sub-divided into $I = 70$ areas. These sub-Regional Health Authorities (sRHAs) are the geographic units used in our analysis, and all data, for both population and cancer cases, are linked to these geographic boundaries.

The number of cancer cases totaled 1,966 over the study period. Of

these, 24 cases have either missing ages or sex entries of other, and hence were removed from the analysis (i.e., our analysis is based on 1,942 cases). The mean and median number of yearly cases per sRHA are 2.8 and 2.4 (ranging from 0.2 to 7.5), respectively. The values of the sRHA population sizes range from 2,458 to 30,560, with mean and median values of 12,140 and 11,720, respectively. Region 52 has the smallest population, and region 50 has the largest. Table 1 reveals that the observed rates of cancer diagnoses were generally increasing over time for both males and females, with rates for males lower than those for females.

“Table 1 about here”

Because gender is not thought to be a predictor of the development of childhood cancers, analyses were stratified by gender. The expected number of cancer cases, e_{it} , was adjusted and calculated as $e_{it} = \sum_{j=1}^4 n_{itj}y_j/n_j$, where j indexes the age group (0-4, 5-9, 10-14, 15-19 years), n_{itj} is the population at risk in sRHA i at time t for age group j , $y_j = \sum_i \sum_t y_{itj}$, and similarly, $n_j = \sum_i \sum_t n_{itj}$. We estimated several spatio-temporal models of equation form (1), to analyze the ratio of cancer diagnoses, using WinBUGS and BOA. For the first step, the simple linear temporal trend model (M1) was considered and defined as $\log(\mu_{it}^c/e_{it}) = m + \beta t$. Estimates of the linear trend effect β indicate an increasing trend (0.026 with standard error 0.010

for females, and 0.014 with standard error 0.012 for males) in the ratio of cancer diagnoses over time for this period. Table 2 reports model M1 as well as other model specifications we thought were appropriate in our exploration of the data. These sub-models of the spatio-temporal model (1) have an increasing level of complexity. For instance, model M2 is the simple linear trend model M1 plus a linear regional (sRHA) temporal component, and spatially structured (η_i) and unstructured (ϕ_i) components. Model M3 essentially is model M2 with the simple linear trend βt replaced with a cubic B-spline $S(t)$. Sub-models of M2 and M3 are variants of the models M2 and M3.

To compare competing models, we calculated the measures of overall fit SD , P , and DIC using the WinBUGS package. On the basis of these values, listed in Table 2, model M3B is better than M2 for both females and males, particularly when compared with M1, which includes no spatial random effects. The model M3B is the best model based on the DIC measure. Evidence exists of both a B-spline temporal trend and spatial variation in the standardized incidence ratio. Model M3, or one of its variants, seems slightly better than model M2 in terms of the overall fit measures, although no striking evidence exists indicating that one of these variants is substantially better than the others. The improvement in fit measures for models M1 to

M3 generally seems to have similar magnitudes for both females and males.

“Table 2 about here”

Fig. 1 portrays the overall crude incidence ratio over time adjusted for age group, $\sum_{i=1}^I y_{it} / \sum_{i=1}^I e_{it}$, and incidence ratios, $\exp(m + \beta t)$ and $\exp(m + S(t))$. Fig. 1 reveals that over the studied period, the cubic B-spline produces smooth estimates of the crude incidence ratios for both females and males. An overall increase in childhood cancer ratios over time also exists, especially for females.

“Fig. 1 about here”

Some risk factors may vary spatially, and to evaluate such spatial dependence, the spatial distribution of the regional effects over time is mapped as $\exp(\delta_i t + \eta_i + \phi_i)$ for model M3, which is automatically calibrated on a common base for the temporal effects. Fig. 2 presents maps of the estimated spatial effects based on the fitted model for females and males, where the regional risk factor of cancer cases corresponds to one selected year. For confidentiality, the year is not shown. Note that the break points in Fig. 2 are chosen for convenience, based on the distribution of the cancer ratios, and that the lowest category includes values ranging from 0.75 to 0.85, and the highest category includes values ranging from 1.15 to 1.92. The overall spatial pattern suggests that

some regions with relatively high cancer ratios for females are located in the north-central part of the province, whereas for males some regions with relatively high cancer ratios are located in the south-central part of the province. For females, in addition to the north-central part of the province, some regions in the south part of the province also have relatively high cancer ratios. Generally, the spatial pattern does not change much over time. Parts of the two largest population centres have the highest estimated cancer ratios. The region between these centres also has relatively high ratios in some of its parts. More investigation may be needed to explore the reasons for seemingly higher cancer ratios in these regions compared to other parts of the province.

“Fig. 2 about here”

“Fig. 3 about here”

Fig. 3 furnishes graphs of the childhood cancer ratio estimates for four selected health regions for females over time. Crude incidence ratios adjusted for age group are defined by y_{it}/e_{it} , whereas the other estimated ratios are calculated as $\exp(\delta_{it} + \eta_i + \phi_i)$. Crude incidence ratio estimates are variable in these sub-regions. As shown in Fig. 3, the ratio of cancer diagnoses has an increasing trend over time in regions shown in panels (b) and (c), and has a decreasing trend in regions shown in panels (a) and (d). Similar

patterns are observed for males (not shown). In general, a certain trend in the log-ratio estimates over time for a region suggests that the underlying rate of cancer cases in that region also has the same pattern relative to the provincial average.

In Bayesian estimation of parameters for the purposes of disease mapping, choosing suitable values for the prior assumptions also is important. Full details of the prior sensitivity and choice of models appear in Pascutto et al. (2000). We investigate the choice of priors through a sensitivity study for the childhood cancer cases in the next section.

Prior sensitivity

The hyperprior distributions of the variance components are generally set to be vague to get the most information from the data. The prior for the precision of the random effects (σ^{-2}) often is specified as a gamma distribution with scale and shape parameters both equal to 0.001. One also may use a uniform prior for the random effects σ^2 . However, when modeling the precision of the spatial random effects in an ICAR model, using a gamma distribution with scale parameter equal to 0.5 and shape parameter equal to 0.0005 (Bernardinelli, Clayton, and Montomoli 1995; Kelsall and Wakefield

1999; Silva et al. 2008) is common.

To investigate the influence of hyperprior specifications in the Poisson context, we conducted a sensitivity analysis with respect to the prior distributions for the spatial precision parameters σ_η^{-2} and σ_ϕ^{-2} , assuming a variety of different gamma priors $G(a, b)$, whose mean and variance are a/b and a/b^2 , respectively. Note that we used the same priors for σ_δ^{-2} and σ_l^{-2} . In our experimental design, similar to Silva et al. (2008), we used the following combinations: $(a, b) = (0.5, 0.0005), (0.001, 0.001), (0.01, 0.01), (0.1, 0.1), (2, 0.001), (0.2, 0.0004)$, and $(10, 0.25)$, which are denoted by A, B, C, D, E, F , and G , respectively. Prior B has a larger dispersion than A , and C and D are variants of prior B , with the associated precision in increasing order. Priors E and F correspond to distributions with the same variance as prior A , but with lower (E) and larger (F) dispersion. Prior G is the furthest departure from a non-informative setting.

Table 3 provides summary measures of model fit for models $M1, M2$, and $M3$ with various hyperparameter settings for gender-specific analyses. The cubic B-spline model seems to provide a better fit than the linear trend for overall time trend, for both females and males. When comparing DIC values across both models and priors, the more striking effect is that the DIC slightly tends to prefer model $M3$ compared to model $M2$, and a smaller difference

exists in the DIC across priors than across models. For the vague priors considered here, omitting the main effects in the model seems to play a more important role than the choice of prior in determining the goodness-of-fit with respect to the DIC and the other measures of fit considered (SD and P). We also considered different combinations of priors ($A - G$) for models $M2$ and $M3$; the results were almost equal regardless of the priors (not shown). As a result, changing the prior assumptions on the variance components does not have a considerable effect on the selected model in the Application section.

“Table 3 about here”

Summary and conclusion

We illustrate a model for spatio-temporal analysis that pays specific attention to the mapping of area-level disease ratios over time. The model accommodates a cubic B-spline for the overall temporal trend, a small-area linear temporal trend, and an ICAR and independent normal random variable models for specified and unspecified spatial random effects, respectively. The fully Bayesian approach is employed for the analysis using MCMC techniques. We studied the convergence of the samples obtained through diagnostic methods, and concluded that convergence was achieved. Our sensitivity analysis using different priors for the variance components points out that

this hierarchical Bayesian spatio-temporal analysis for Poisson data yields similar results regardless of the vague priors considered in the Application section.

We used a B-spline for this Bayesian spatio-temporal analysis, which can be easily incorporated into the modeling of the temporal components, and which is computationally straightforward. However, we could not apply the B-spline approach for each specific region, $S_i(t)$, because of an insufficient number of observations, and, consequently, unidentifiability of the associated model parameters.

We adjusted our expected number of cases by age. One can easily extend the approach to include covariates in the model specification, and such an inclusion may be required for some applications. However, the total number of cancer cases in our data set limited our ability to include such covariates directly. More precisely, in order to include the covariates in the model, one needs to have more observations to ensure valid inference. In addition, the relative rarity of childhood cancer means that diagnosis-specific (i.e., leukemia, lymphoma) types could not be separately analyzed. This aspect may be a considerable limitation if different diagnosis-specific risk factors exist that vary over geography. A study in a larger geographical region with additional years may be necessary for diagnosis-specific analyses.

Overall, the model estimates suggest that the childhood cancer incidence ratios are increasing over time for both females and males. For females, the north-central part of the province has generally higher ratios than the other areas, although some regions in the south part of province also have higher ratios. Moreover, the south-central part of the province generally has higher ratios than other areas for males. These findings may represent real increases, or may represent different distributions of important covariates that are unmeasured and unadjusted for in our modeling. Further investigation may be warranted to explore these findings. In the United States and Europe, the overall rates of childhood cancer have increased since the 1970s (Ries et al. 1999; McKinney et al. 2003; Dreifaldt, Carlberg, and Hardell 2004; Steliarova-Foucher, Stiller, and Kaatsch 2004; Dalmasso et al. 2005), which collaborate the notion of real increases here.

Acknowledgements

M. Torabi was supported by a Full-time Fellowship Award from Alberta Heritage Foundation for Medical Research (AHFMR). R.J. Rosychuk is supported by AHFMR as a Health Scholar. The authors thank the Alberta Cancer Registry for providing the cancer data and Alberta Health and Wellness for providing the population data. We thank the editor and three referees for

the valuable comments that have substantially improved an earlier version of this article.

Disclaimer: The interpretations, conclusions and opinions expressed in this paper are those of the authors and do not necessarily reflect the position of the Alberta Cancer Board. This study is based in part on data provided by Alberta Health and Wellness. The interpretation and conclusions contained herein are those of the researchers and do not necessarily represent the views of the Government of Alberta. Neither the Government nor Alberta Health and Wellness express any opinion in relation to this study.

References

Banerjee, S., B.P. Carlin, and A.E. Gelfand. (2004). *Hierarchical Modeling and Analysis for Spatial Data*. Chapman and Hall/CRC: London/Boca Raton, FL.

Bernardinelli, L., D. Clayton, and C. Montomoli. (1995). “Bayesian Estimates of Disease Maps: How Important Are Priors?” *Statistics in Medicine* 14, 2411-31.

Bernardinelli, L., D. Clayton, C. Pascutto, C. Montomoli, and M. Ghislandi. (1995). “Bayesian Analysis of Space-Time Variation in Disease Risk.” *Statistics in Medicine* 14, 2433-43.

Bernardinelli, L., and C. Montomoli. (1992). “Empirical Bayes Versus Fully

Bayesian Analysis of Geographical Variation in Disease Risk.” *Statistics in Medicine* 11, 983-1007.

Besag, J., and C.L. Kooperberg. (1995). “On Conditional and Intrinsic Autoregressions.” *Biometrika* 82, 733-46.

Besag, J., J. York, and A. Mollié. (1991). “Bayesian Image Restoration, with Two Applications in Spatial Statistics.” *Annals of Institute of Statistical Mathematics* 43, 1-21.

Best, N.G., R.A. Arnold, A. Thomas, L.A. Waller, and E.M. Conlon. (1999). “Bayesian Models for Spatially Correlated Disease and Exposure Data (with Discussion).” In *Bayesian Statistics 6*, 131-56, edited by J.M. Bernardo, J.O. Berger, A.P. Dawid and A.F.M. Smith. Oxford University Press.

Borugian, M.J., J.J. Spinelli, G. Mezei, R. Wilkias, Z. Abanto, and M.L. McBride. (2005). “Childhood Leukemia and Socioeconomic Status in Canada.” *Journal of Epidemiology* 16, 526-31.

Breslow, N.E., and D.G. Clayton. (1993). “Approximate Inference in Generalized Linear Mixed Models.” *Journal of American Statistical Association* 88, 9-25.

Breslow, N.E., and X. Lin. (1995). “Bias Correction in Generalized Linear Mixed Models with a Single Component of Dispersion.” *Biometrika* 82(1), 81-91.

- Brooks S., and A. Gelman. (1998). "General Methods for Monitoring Convergence of Iterative Simulations." *Journal of Computational and Graphical Statistics* 7(4), 434-55.
- Clayton, D.G., and L. Bernardinelli. (1992). Bayesian Methods for Mapping Disease Risk. In *Geographical and Environmental Epidemiology: Methods for Small-Area Studies*, 205-20, edited by P. Elliott, J. Cuzick, D. English and R. Stern. Oxford: Oxford University Press.
- Clayton, D.G, and J. Kaldor. (1987). "Empirical Bayes Estimates of Age-Standardized Relative Risks for Use in Disease Mapping." *Biometrics* 43, 671-81.
- Cressie, N. (1992). "Smoothing Regional Maps Using Empirical Bayes Predictors." *Geographical Analysis* 24, 75-95.
- Dalmasso, P., G. Pastore, L. Zuccolo, M.M. Maule, N. Pearce, F. Merletti, and C. Magnani. (2005). "Temporal Trends in the Incidence of Childhood Leukemia, Lymphomas and Solid Tumors in North-West Italy, 1967-2001. A Report of the Childhood Cancer Registry of Piedmont." *Hematology Journal* 90(9), 1197-1204.
- De Boor, C. (1978). *A Practical Guide to Splines*. New York: Springer-Verlag.
- Dean, C.B., M.D. Ugarte, and A.F. Militino. (2004). "Penalized Quasi-Likelihood with Spatially Correlated Data." *Computational Statistics and Data Analysis* 45, 235-48.

- Dreifaldt, A.C., M. Carlberg, and L. Hardell. (2004). "Increasing Incidence Rates of Childhood Malignant Diseases in Sweden During the Period 1960-1998." *European Journal of Cancer* 40, 1351-60.
- Earnest, A., G. Morganl, K. Mengersen, L. Ryan, R. Summerhayes, and J. Beard. (2007). "Evaluating the Effect of Neighbourhood Weight Matrices on Smoothing Properties of Conditional Autoregressive (CAR) Models." *International Journal of Health Geographics* 6:54.
- Eilers, P.H.C., and B.D. Marx. (1996). "Flexible Smoothing with B-splines and Penalties." *Statistical Science* 11(2), 89-121.
- Gelfand, A.E., and A.F.M. Smith. (1990). "Sampling-Based Approaches to Calculating Marginal Densities." *Journal of American Statistical Association* 85, 398-409.
- Gelman, A., and D.B. Rubin. (1992). "Inference from Iterative Simulation Using Multiple Sequences (with Discussion)." *Statistical Science* 7, 457-511.
- Harville, D.A. (1997). *Matrix Algebra from a Statistician's Perspective*. Springer, New York.
- Heidelberger P., and P. Welch. (1983). "Simulation Run Length Control in the Presence of an Initial Transient." *Operations Research* 31, 1109-44.
- Kelsall, J.E., and J.C. Wakefield. (1999). Discussion of "Bayesian Models for Spatially Correlated Disease and Exposure Data" by Best, N.G., L.A.

Waller, A. Thomas, E.M. Conlon, and R. Stern. In *Bayesian Statistics 6*, edited by J.M. Bernardo, J.O. Berger, A.P. Dawid and A.F.M. Smith. Oxford University Press: Oxford.

Knorr-Held, L. (2000). “Bayesian Modeling of Inseparable Space-Time Variation in Disease Risk.” *Statistics in Medicine* 19, 2555-67.

Leroux, B.G., X. Lei, and N. Breslow. (1999). Estimation of Disease Rates in Small Areas: A New Mixed Model for Spatial Dependence. In *Statistical Models in Epidemiology, the Environment and Clinical Trials*, 135-78, edited by M.E. Halloran and D. Berry. New York: Springer-Verlag.

Liang, K.Y., and S.L. Zeger. (1986). “Longitudinal Data Analysis Using Generalized Linear Models.” *Biometrika* 73, 13-22.

Lin, X., and N.E. Breslow. (1996). “Bias Correction in Generalized Linear Mixed Models with Multiple Components of Dispersion.” *Journal of American Statistical Association* 91, 1007-16.

Lu, H., and Carlin, B.P. (2005). “Bayesian Areal Wombling for Geographical Boundary Analysis.” *Geographical Analysis* 37, 265-285.

Lunn, D.J., A. Thomas, N. Best, and D. Spiegelhalter. (2000). “WinBUGS- A Bayesian Modelling Framework: Concepts, Structure, and Extensibility.” *Statistics and Computing* 10, 325-37.

- MacNab, Y.C., and C.B. Dean. (2000). "Parametric Bootstrap and Penalized Quasi-Likelihood Inference in Conditional Autoregressive Models." *Statistics in Medicine* 19 (17/18), 2421-35.
- MacNab, Y.C., and C.B. Dean. (2001). "Autoregressive Spatial Smoothing and Temporal Spline Smoothing for Mapping Rates." *Biometrics* 57, 949-56.
- Martinez-Beneito, M.A., A. López-Quilez, and P. Botella-Rocamora. (2008). "An Autoregressive Approach to Spatio-Temporal Disease Mapping." *Statistics in Medicine* 27, 2874-89.
- McCullagh, P., and J.A. Nelder. (1989). *Generalized Linear Models* (2nd edn). London: Chapman and Hall.
- McKinney, P.A., R.J. Feltbower, R.C. Parslow, I.J. Lewis, A.W. Glaser, and S.E. Kinsey. (2003). "Patterns of Childhood Cancer by Ethnic Group in Bradford, UK 1974-1997." *European Journal of Cancer* 39, 92-7.
- Pascutto, C., J.C. Wakefield, N.G. Best, S. Richardson, L. Bernardinelli, A. Staines, and P. Ellitt. (2000). "Statistical Issues in the Analysis of Disease Mapping Data." *Statistics in Medicine* 19, 2493-2519.
- Prentice, R.L., and L.P. Zhao. (1991). "Estimating Equations for Parameters in Means and Covariances of Multivariate Discrete and Continuous Responses." *Biometrics* 47, 825-39.

R Development Core Team: A Language and Environment for Statistical Computing. R Foundation for Statistical Computing. <http://www.R-project.org>.

Ries, L.A.G., M.A. Smith, J.G. Gurney, M. Linet, T. Tamra, J.L. Young, and G.R. Bunin.(eds.) (1999). "Cancer Incidence and Survival Among Children and Adolescents: United States SEER Program 1975-1995," *Bethesda (MD): National Cancer Institute, SEER Program*. NIH Pub. No. 99-4649.

Silva, G.L., C.B. Dean, T. Niyonsenga, and A. Vanasse. (2008). "Hierarchical Bayesian Spatiotemporal Analysis of Revascularization Odds Using Smoothing Splines." *Statistics in Medicine* 27, 2381-2401.

Smith, B.J. (2007). *BOA User Manual (version 1.1.7)*. Department of Biostatistics, College of Public Health, University of Iowa, Ames, IA.

Spiegelhalter, D.J., N.G. Best, B.P. Carlin, and A. Van der linde. (2002). "Bayesian Measures of Model Complexity and Fit." *Journal of Royal Statistical Society Ser. B* 64, 583-639.

Steliarova-Foucher, E., C. Stiller, and P. Kaatsch. (2004). "Geographical Patterns and Time Trends of Cancer Incidence and Survival Among Children and Adolescents in Europe Since the 1970s (the ACCIS project): An Epidemiological Study." *Lancet* 364, 2097-2105.

The North American Association of Central Cancer Registries. <http://www.naaccr.org/>. Accessed September 24, 2010.

Waller, L.A., B.P. Carlin, H. Xia, and A.E. Gelfand. (1997). “Hierarchical Spatio-Temporal Mapping of Disease Rates.” *Journal of American Statistical Association* 92, 607-17.

Wheeler, D.C., D.A. Hickson, and L.A. Waller. (2010). “Assessing Local Model Adequacy in Bayesian Hierarchical Models Using the Partitioned Deviance Information Criterion.” *Computational Statistics & Data Analysis* 54(6), 1657-71.

Zeger, S.L. (1988). “A Regression Model for Time Series of Counts.” *Biometrika* 75, 621-29.

Table 1 Observed Rates (per 1,000 children) of Cancer Diagnoses for Females and Males During 1995-2004

| Gender | 1995 | 1996 | 1997 | 1998 | 1999 | 2000 | 2001 | 2002 | 2003 | 2004 |
|--------|------|------|------|------|------|------|------|------|------|------|
| Female | 0.22 | 0.28 | 0.24 | 0.24 | 0.30 | 0.26 | 0.30 | 0.30 | 0.28 | 0.33 |
| Male | 0.17 | 0.17 | 0.17 | 0.19 | 0.11 | 0.17 | 0.18 | 0.17 | 0.19 | 0.23 |

Table 2 The Values of P , SD , and DIC for Comparison of the Sub-Models of Model (1)

| Gender | Models defined from $\log(\mu_{it}^e/e_{it})$ | P | SD | DIC |
|---|---|--------------------|------|-------|
| Female | $M1 : m + \beta t$ | 1112 | 485 | 496 |
| | $M2 : m + \beta t + \delta_i t + \eta_i + \phi_i$ | 736 | 407 | 417 |
| | $M2A : m + \beta t + \eta_i + \phi_i$ | 740 | 409 | 417 |
| | $M2B : m + \beta t + \delta_i t + \eta_i$ | 735 | 406 | 425 |
| | $M2C : m + \beta t + \delta_i t + \phi_i$ | 733 | 405 | 426 |
| | $M3 : m + S(t) + \delta_i t + \eta_i + \phi_i$ | 728 | 395 | 412 |
| | $M3A : m + S(t) + \eta_i + \phi_i$ | 736 | 408 | 415 |
| | $M3B : m + S(t) + \delta_i t + \eta_i$ | 722 | 385 | 402 |
| | $M3C : m + S(t) + \delta_i t + \phi_i$ | 731 | 405 | 423 |
| | Male | $M1 : m + \beta t$ | 1351 | 511 |
| $M2 : m + \beta t + \delta_i t + \eta_i + \phi_i$ | | 675 | 309 | 317 |
| $M2A : m + \beta t + \eta_i + \phi_i$ | | 677 | 309 | 318 |
| $M2B : m + \beta t + \delta_i t + \eta_i$ | | 676 | 309 | 326 |
| $M2C : m + \beta t + \delta_i t + \phi_i$ | | 674 | 309 | 327 |
| $M3 : m + S(t) + \delta_i t + \eta_i + \phi_i$ | | 672 | 295 | 310 |
| $M3A : m + S(t) + \eta_i + \phi_i$ | | 677 | 308 | 314 |
| $M3B : m + S(t) + \delta_i t + \eta_i$ | | 667 | 287 | 302 |
| $M3C : m + S(t) + \delta_i t + \phi_i$ | | 675 | 308 | 323 |

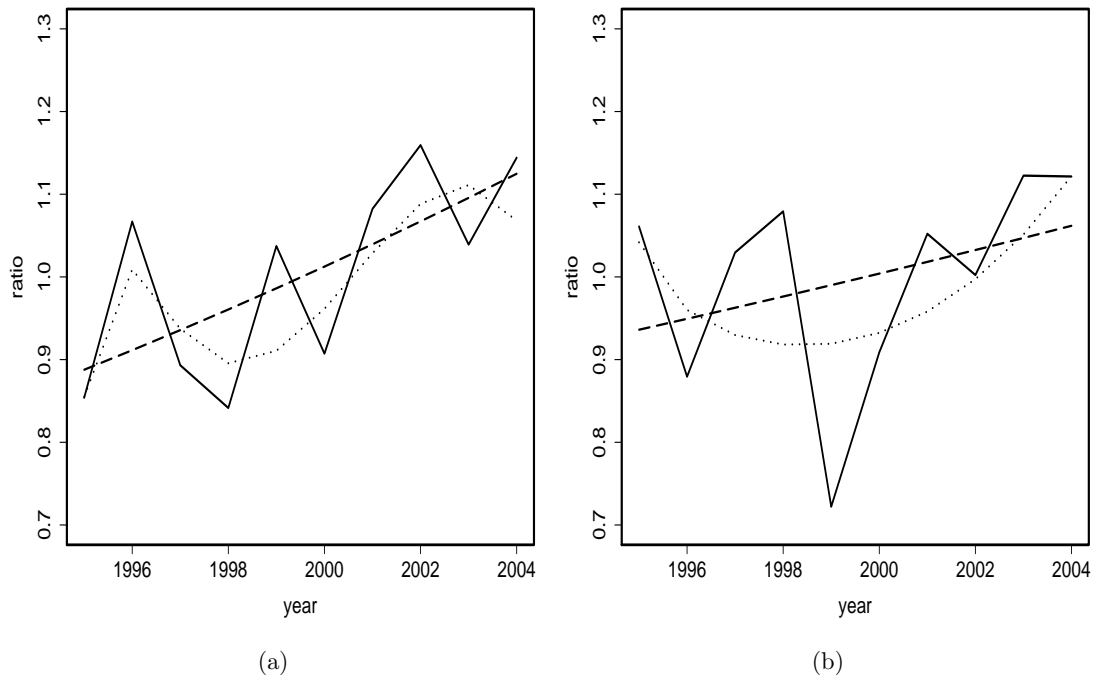


Figure 1. Overall childhood cancer incidence ratios over time for (a) females and (b) males (crude incidence ratio [solid line], linear trend [dashed line], cubic B-spline [dotted line]).

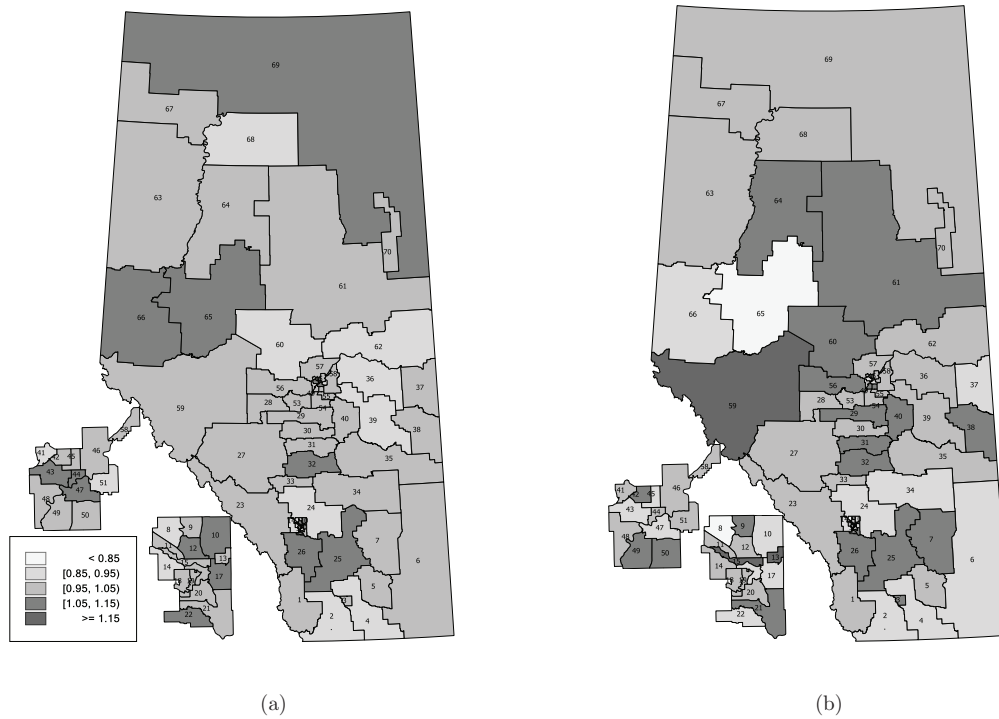


Figure 2. Maps of the childhood cancer incidence ratios corresponding to the spatial effects representing regional incidence risks for (a) females and (b) males for one selected year; Alberta childhood cancer data, 1995-2004. Major urban areas are provided as inserts.

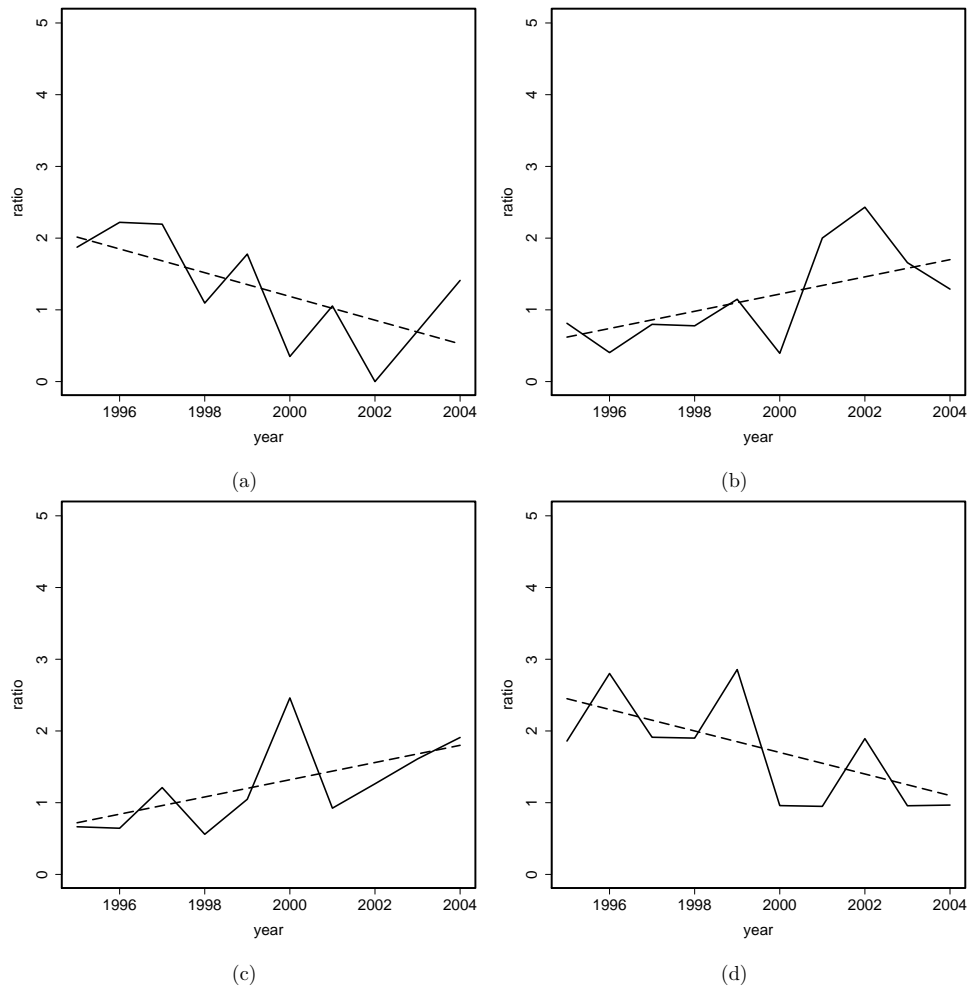


Figure 3. Plots of crude incidence ratio estimates and estimated ratios based on model M3 for females, 1995-2004, for local health regions 6, 17, 22, and 65 in plots (a), (b), (c), and (d), respectively. The solid line represents crude incidence ratios; the dashed line, fitted ratios.

Table 3 The Values of P , SD , and DIC for Sensitivity Analysis of the Model Selection

| Prior | Models | Females | | | Males | | |
|-------|--------|---------|------|-------|-------|------|-------|
| | | P | SD | DIC | P | SD | DIC |
| A | $M1$ | 1112 | 485 | 496 | 1351 | 511 | 530 |
| | $M2$ | 736 | 407 | 417 | 675 | 309 | 317 |
| | $M3$ | 728 | 395 | 412 | 672 | 295 | 310 |
| B | $M2$ | 734 | 410 | 416 | 674 | 309 | 317 |
| | $M3$ | 726 | 398 | 411 | 671 | 295 | 310 |
| C | $M2$ | 732 | 408 | 415 | 673 | 308 | 317 |
| | $M3$ | 724 | 396 | 410 | 669 | 293 | 308 |
| D | $M2$ | 724 | 496 | 414 | 669 | 301 | 317 |
| | $M3$ | 717 | 384 | 410 | 666 | 286 | 310 |
| E | $M2$ | 740 | 418 | 417 | 678 | 314 | 319 |
| | $M3$ | 728 | 405 | 412 | 674 | 299 | 311 |
| F | $M2$ | 736 | 412 | 416 | 675 | 310 | 318 |
| | $M3$ | 726 | 399 | 411 | 672 | 296 | 309 |
| G | $M2$ | 727 | 404 | 418 | 667 | 303 | 318 |
| | $M3$ | 722 | 400 | 416 | 664 | 287 | 310 |